Visualization of the space-time impulse response of the subcritical wake of a cylinder

P. Le Gal[1] and V. Croquette[2]
[1]*Institut de Recherche sur les Phénomènes Hors Equilibre, UM 6594, Universités d'Aix-Marseille I and II-CNRS, 12 Avenue Général Leclerc, 13003 Marseille, France*
[2]*Ecole Normale Supérieure, Laboratoire de Physique Statistique, URA 1306, Universités de Paris 6 and 7-CNRS, 24 Rue Lhomond, 75005 Paris, France*
(Received 6 March 2000)

The well-known Bénard–von Kàrmàn cylinder wake is one of the most challenging phenomena of fluid mechanics. As the Reynolds number of the flow around a cylinder passes through a critical value, alternating vortex shedding appears via a Hopf bifurcation. Theoretical studies of the wake have described the appearance of this self-sustained oscillation as the result of a convective to absolute transition resulting in the formation of a global mode. We illustrate here the convective global regime of the subcritical wake by analyzing visualizations of its impulse response.

PACS number(s): 47.20.−k, 47.27.Vf

Since the seminal work of Bénard at the beginning of the century [1], the alternate vortex shedding of the wake of a cylinder has continually attracted fluid dynamicists. Many impressive visualizations have been obtained in wind or water tunnels and have appeared in many publications (e.g., [2]). But complete understanding of the instability which causes growth and shedding of the vortex street is still not complete. One of the oldest analyses was performed by von Kàrmàn [3], who described the cylinder wake by a double row of point vortices. This approach was continued by Kida [4], but more significant progress was in fact obtained by linear stability analyses of the wake [5,6]. The appearance of self-sustained oscillations was finally interpreted by means of results originally obtained in plasma physics [7,8]. In this context, it was possible to establish the link between local linear analysis of velocity profiles [9] and global oscillating modes of wakes [10,11]. Contrary to two-dimensional analyses that use linearized Navier-Stokes equations to determine the criteria of stability of 2D flows [12], local analyses make the assumption of locally parallel flows in the streamwise direction. At each streamwise position, a linear stability analysis is used to determine the local nature of the instability. The flow is then said to be absolutely unstable if its impulse response grows in time at the considered location, and convectively unstable if the impulse response grows while propagating downstream. In other words, the instability is absolute if the mode with a null group velocity (versus the cylinder) has a positive growth rate. These concepts lead also to the definition of criteria for the frequency selection of the global mode [13]. Using the Orr-Sommerfeld equation, Monkewitz showed [10] that, above a threshold (Reynolds number $\mathrm{Re}_a = 25$), there is a region of absolute instability downstream from the cylinder which needs to be large enough for the instability to become global. These results have then been further analyzed in the framework of the complex Ginzburg-Landau equation by Chomaz *et al.* [14] and Le Dizès *et al.* [15] and verified by Hammond and Redekopp in direct numerical simulations of wake-shear layers [16]. More recently, a nonlinear extension was obtained [17], and the criteria that distinguish the absolute from the convective type of instability were revisited and expressed in terms of propagating front velocities [18,19]. These essential properties of wake behavior are usually illustrated by space-time diagrams showing the advection and diffusion of a wave packet [11]. The goal of this work is to present an illustration of the impulse response of the cylinder wake in the convective regime of the global instability, that is, below the vortex shedding threshold, which is around $\mathrm{Re} = 47$ for a sufficiently long cylinder. The study of the impulse response of the subcritical wake is a classical procedure for analyzing the critical slowing down near the Hopf bifurcation [20–23], but to our knowledge, this is the first time that it is the subject of an experimental spatiotemporal analysis.

Our experiment was realized in a vertical water tunnel with a 200 mm side square section. The stainless steel cylinder has a diameter of 2 mm and is fixed rigidly through a groove in the wall of the tunnel on a displacement system in such a way that its free end is very close (1/10 mm) to the opposite window. Therefore, the effective length of the cylinder is 200 mm and we emphasize that no end plates have been used in order to control parallel vortex shedding [24]. The wakes were visualized by a white silicon emulsion (Rhodorsil), which can be gently emitted through a 0.05 mm diameter hole, drilled at midlength in the rear face of the cylinder. The Reynolds number Re of the wake, based on the diameter of the cylinder, is adjusted by controlling the flow rate in the tunnel. The visualizations presented in Fig. 1 are obtained for a Reynolds number $\mathrm{Re} = 35$ (corresponding to a velocity of 17.5 mm/s), which is less than the global mode threshold. Despite the fact that we study a streak-line deformation and not the velocity field, we will see that no locally absolutely unstable behavior is detected in the wake, although the excitation is done in a regime and in a region of the wake where the dynamics is absolutely unstable [10].

When the flow is not perturbed, the streak line is a straight vertical line except in the recirculation eddies just downstream of the cylinder. But, as soon as the cylinder is very slightly displaced in a single back and forth rapid motion of a tenth of a millimeter, a wave packet is generated and advected downstream. The series of photographs presented in

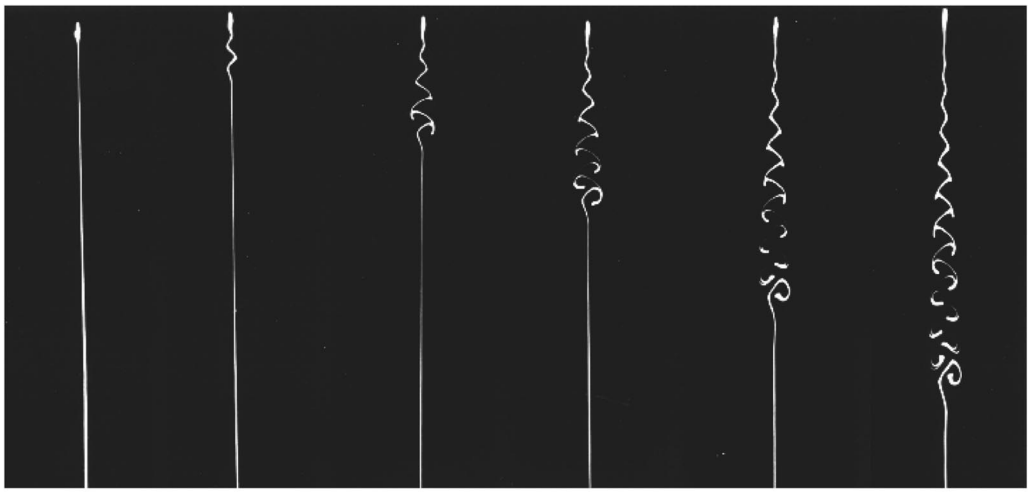

FIG. 1. Visualization of the spatiotemporal impulse response of the cylinder wake. Re=35. There is a time lapse (vertical axis) between each photograph of around 3 sec.

Fig. 1 shows the deformation of the white streak line caused by the evolution of this wave packet. As can be seen, the dye filament presents first a slight undulation in the near wake and finally is rolled up by the flow. For a very small perturbation (less than one-tenth of a millimeter), we can realize a real-time video analysis, unimpeded by this roll-up. For this purpose, an analog device was built in order to record directly the shape of the dye streak [25]. The output analog signal is composed of a succession of dye filament profiles. These profiles, each consisting of 256 data points in the longitudinal X direction, corresponding to a total length of 18.2 cm, are recorded by a microcomputer by a standard acquisition chain. One of these profiles is given in Fig. 2, where it can be noted that the dye filament deformation wave grows linearly with space and where the wavelength evolves from 18 mm near the cylinder to 21 mm in the far wake. By piling up these successive profiles, space-time diagrams can be easily constructed. Figure 3 shows such a diagram representing the evolution of the wave packet for a series of video images having a total duration of 24 sec. The gray level represents the amplitude $A(X,t)$ of the dye deformation. The convective nature of the wake is made clearly. As the Reynolds number approaches the global instability threshold, this rear front would be expected to propagate more slowly (its angle with the vertical time axis will be smaller). When reaching the Bénard–von Kàrmàn instability threshold, the phase velocity of this edge should then vanish. We emphasize that the recorded pattern is relative to the deformation of the streak line and not to the velocity field directly, in contrast to the numerical simulation results presented in [17]. In particular, although the amplitude of the streak-line deformation is obviously linked to the amplitude of the velocity fluctuations, a direct relation between these two fields is far from being established. However, the analysis of the pattern determines a shedding frequency $f=0.75$ Hz, which corresponds to a Strouhal number close to 0.08. The phase velocity evolves from 13 mm/s near the cylinder to 16 mm/s (90% of the fluid velocity) in the far wake. This feature generates a very slight curvature of the isophase lines, as can be observed in Fig. 3. We remark also that no waves are generated at the leading edge of the wave packet, as observed in the numerical simulation of Delbende and Chomaz [17], in the case of a nonconfined wake.

We are grateful to S. Le Dizès for stimulating discussions and to A. Morand for the photographic work.

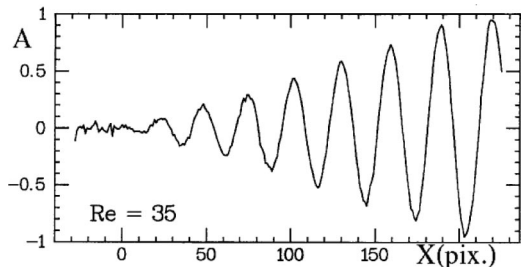

FIG. 2. Dye streak profile at time $t=14.5$ s. Re=35. The amplitude A of the dye filament deformation is in arbitrary units.

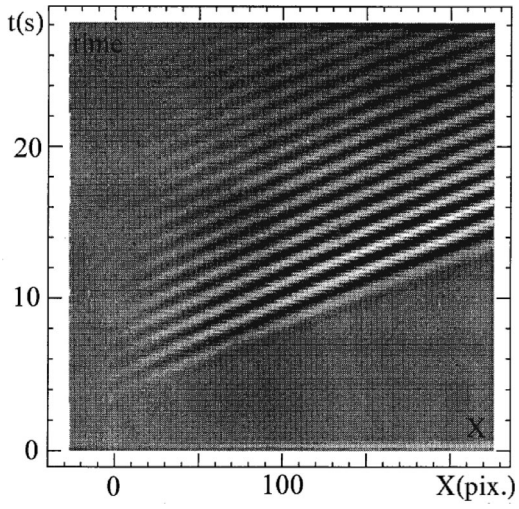

FIG. 3. Space-time diagram $A(X,t)$ of the dye streak pattern of the impulse response of the cylinder wake. Re=35. Time is in seconds.

[1] H. Bénard, C. R. Acad. Sci. **147**, 839 (1908).
[2] M. Van Dyke, *An Album of Fluid Motion* (The Parabolic Press, Stanford, CA, 1982).
[3] T. von Kàrmàn, *Uber den Mechanismus der Widerstander den ein bewegter Körper in einer Flüsseigkeit afahrt* (Gott. Nachr., 1911), p. 509.
[4] S. Kida, J. Fluid Mech. **122**, 487 (1982).
[5] R. Betchkov and W. Criminale, Phys. Fluids **9**, 359 (1966).
[6] G. E. Mattlingly and W. O. Criminale, J. Fluid Mech. **51**, 233 (1972).
[7] R. Briggs, *Electron-Stream Interaction with Plasmas* (MIT Press, Cambridge, MA, 1964).
[8] A. Bers (unpublished).
[9] X. Yang and A. Zebib, Phys. Fluids A **1**, 689 (1989).
[10] P. A. Monkewitz, Phys. Fluids **31**, 999 (1988).
[11] P. Huerre and P. A. Monkewitz, Annu. Rev. Fluid Mech. **22**, 473 (1990).
[12] C. P. Jackson, J. Fluid Mech. **182**, 23 (1987).
[13] W. Koch, J. Sound Vib. **41**, 53 (1985).
[14] J. M. Chomaz, P. Huerre, and L. G. Redekopp, Phys. Rev. Lett. **60**, 25 (1988).
[15] S. Le Dizès, P. Huerre, J. M. Chomaz, and P. A. Monkewitz, Philos. Trans. R. Soc. London, Ser. A **354**, 169 (1996).
[16] D. A. Hammond and L. G. Redekopp, J. Fluid Mech. **331**, 231 (1997).
[17] I. Delbende and J. M. Chomaz, Phys. Fluids **10**, 2724 (1998).
[18] G. Dee and J. S. Langer, Phys. Rev. Lett. **50**, 383 (1983).
[19] W. Van Saarlos, Phys. Rev. A **37**, 211 (1988).
[20] M. Provansal, C. Mathis, and L. Boyer, J. Fluid Mech. **182**, 1 (1987).
[21] J. Dusek, P. Le Gal, and Ph. Fraunié, J. Fluid Mech. **264**, 59 (1994).
[22] M. Schumm, E. Berger, and P. Monkewitz, J. Fluid Mech. **271**, 17 (1994).
[23] I. Peschard, P. Le Gal, and Y. Takeda, Exp. Fluids **26**, 12 (1999).
[24] C. H. K. Williamson, J. Fluid Mech. **206**, 579 (1989).
[25] P. Le Gal and V. Croquette, Bull. S.F.P. **81**, 29 (1991).